# Improved Accuracy in Susceptibility-based OEF Measurements by Mitigation of Partial-Volume Effects via Combined Magnitude and Phase Reconstruction

Patrick McDaniel[1], Audrey Fan[2], Berkin Bilgic[3], Jeffrey N. Stout[4], and Elfar Adalsteinsson[1,4]

*[1]Electrical Engineering and Computer Science, Massachusetts Institute of Technology, Cambridge, MA, United States, [2]Radiology, Richard M. Lucas Center for Imaging, Stanford University, Stanford, CA, United States, [3]A. A. Martinos Center for Imaging, Department of Radiology, Massachusetts General Hopsital, Charlestown, MA, United States, [4]Health Sciences and Technology, Harvard-MIT, Cambridge, MA, United States*

**Target Audience:** Scientists and physicians who are interested in quantification of magnetic susceptibility and brain oxygenation

**Intro**: Quantitative Oxygen Extraction Fraction (OEF) measurements in the brain can be used to monitor tumor progression[1] and stratify stroke risk. MRI phase images allow for estimation of magnetic susceptibility in veins, from which venous OEF is calculated[2]. This approach is inherently demands high spatial resolution to isolate venous blood inside vessels, and to avoid partial-volume artifacts that may compromise the accuracy of OEF estimates. This consideration is especially relevant in clinical scans, where limited scan time constrains the achievable image resolution. Here, we propose a method to mitigate partial volume effects in quantitative susceptibility mapping (QSM) of venous blood signal through incorporation of the T2*-weighted magnitude signal that accompanies the acquired phase image[3]. We call this method the Magnitude and Phase (MP) Method.

**Methods**: The proposed MP method exploits the full complex-valued MRI signal, to estimate and remove partial-volume effects on phase values in venous blood. We model voxels of interest as comprising two distinct compartments of tissue: one of "vein," and one of "parenchyma," such that the total signal within a voxel is the weighted average of the complex-valued signals of its constituent tissue compartments. In this model, there are two unknown parameters: (1) the underlying venous blood susceptibility ("$\chi_v$"), and (2) the fraction "α" that characterizes the amount of partial volume effect in the voxel. From the acquired complex-valued image, there are two measurements at each voxel: the magnitude "$I_m$" and phase "$\phi_m$". These two measurements together determine a point in (α, $\chi_v$)-space, allowing both parameters to be determined from a ($I_m$, $\phi_m$) measurement (Figure 1). Once $\chi_v$ is known, OEF is quantified via the relationship: $OEF = \chi_v/(4 * pi * \chi_{do} * Hct)$[4].

**Experiments**: The MP method was validated on both numerical and in vivo data. In a numerical model, veins with a known OEF=0.3 were convolved with the dipole kernel that produces a $\Delta B_0$ map, which in turn was used to generate a synthetic map of complex-valued signal. Complex Gaussian noise was added such that SNR=10, and the map was cropped in k-space to simulate a low-resolution MR acquisition. Venous susceptibility was measured by (1) direct measurement from the phase image, (2) by direct measurement from a regularized QSM reconstruction, and (3) by the MP method. The MP method was also tested on previously published, in vivo GRE data with isotropic resolution of 0.6mm[5]. These images were cropped in k-space with different windowing functions (rect and sinc) and window sizes to test the effect of k-space apodization with different window shapes and at various voxel sizes (Figure 3). Pial veins were manually identified and in vivo OEF measurements were obtained by the three approaches described above.

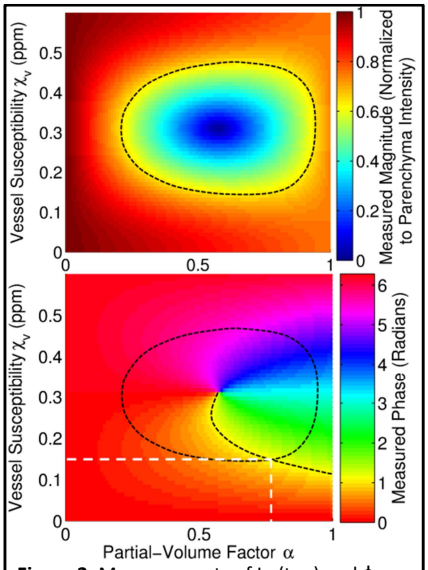


**Figure 2**: Measurements of $I_m$ (top) and $\phi_m$ (bottom) determine a value of (α, $\chi_v$)

**Figure 2**: Simulated vessel OEF measurements compared to ground truth (OEF = 0.3)

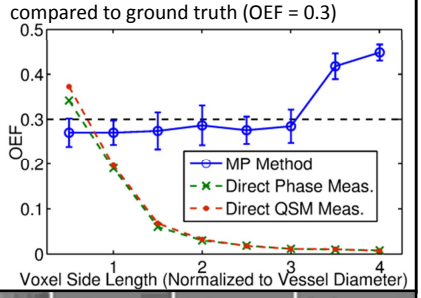


**Results**: In simulation, the MP method produced accurate susceptibility measurements for voxel sizes up to 3 times the vessel diameter at SNR=10, while direct measurement with phase-only reconstruction produced accurate measurements only for voxel dimensions less than or equal to the vessel diameter (Figure 2). Over a range of voxel dimensions from ½ to 3 times the vessel diameter, the average bias from ground truth was -7.6%. On the in vivo data, sinc and rectangular k-space apodization windows yielded OEF measurements that differed from each other by 1.1% for 1.2mm$^3$ voxel size, and 6.3% for 2.4mm$^3$ voxel size. OEF measurements in pial veins (Figure 3) by the MP method were within the physiologically expected range (0.36 to 0.42) for voxel sizes up to twice the vessel diameter, whereas the direct measurements underestimated OEF by over 80% for voxels larger than vessel diameter (Figure 4).

**Discussion**: With the new method, for an SNR of 10, accurate OEF estimates are obtained with less than 7.6% bias even where the voxel dimension is three times the diameter of the vein of interest. For voxel sizes greater than the vessel diameter, these measurements are more accurate than those obtained directly from phase maps or from susceptibility maps. Measurement differences due to k-space apodization window were less than the mean difference from ground truth in simulation.

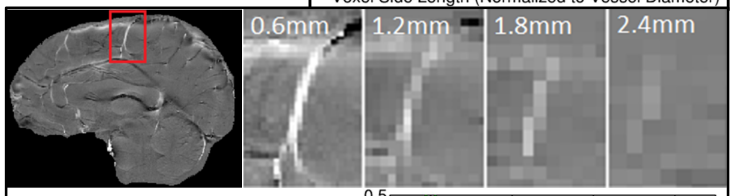


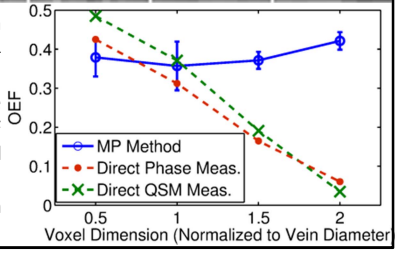


**Figure 3** (top): Pial vessel shown in a sagittal section and close-up at 4 different resolutions. **Figure 4** (right): Comparison of OEF values from the MP method with direct OEF measurements on phase and susceptibility maps. Diameter of vein in Figure 3 was estimated at 1.2mm for normalization.

**Conclusion**: The MP method has the potential to provide more accurate measurements of OEF in narrow pial vessels from susceptibility-based imaging when voxel size is up to 3 times vessel diameter. After partial volume correction, multiple voxels can yield useful OEF measurements. Future work will look to integrate the proposed model into QSM reconstruction methods for veins of arbitrary geometry.

**References**: **[1] Davda** *et al.* (2006) Cancer Metastasis Rev. 25(3): 469-480**. [2] Wang** *et al.* (2014) MRM. DOI: 10.1002/mrm.25358. **[3] Haacke** *et al*. (2009) AJNR 30: 19-30. **[4] Schweser** *et al*. (2011) NeuroImage 54(4): 2789-2807. **[5] Fan** *et al.* (2013) MRM 72(1): 149–159. **Acknowledgements**: R01EB017337